General Procedure for Analysis of the Products of Aprotic Diazotization of Substituted Aryl Alkyl Sulfoxides or Substituted Aryl Alkyl Sulfones. A solution of substituted aryl alkyl sulfoxide or corresponding sulfone (2.5 mmol) and isoamyl nitrite (1 mL, 7.5 mmol) each in glyme (3 mL) was added simultaneously in 1 h to a refluxing solution of trapping agent (1.25 mmol) in glyme (7 mL). After the addition was complete, the mixture was refluxed for 20-30 min and then allowed to cool. Dichloromethane (40 mL) was added, and the mixture was evaporated to dryness. The residual solid was purified by column chromatography as described previously to yield appropriate dihydroanthracene, **12** or **13**, and diphenylene (**11**) or dibenzo-1,4-thioxine (**10**).

General Procedure for Analysis of the Products of Aqueous Diazotization of Substituted Aryl Alkyl Sulfoxides, Substituted Aryl Alkyl Sulfones, or Substituted Aryl Alkyl Thioethers. A solution of substituted aryl alkyl sulfoxide, substituted aryl alkyl sulfone, or substituted aryl alkyl thioether (2 mmol) in dichloromethane (10 mL) and hydrochloric acid or hydrobromic acid (2 mL) was cooled to -10 °C, and solid sodium nitrite (4 mmol) was added slowly in portions. The temperature was maintained at -5 to 0 °C for 3 h. Samples were withdrawn with a microliter syringe and analyzed by GC HP-5840 and Hewlett-Packard GCMS with mass selective detector Model 5920 as described previously.[1-3]

EPR Spectroscopy. The spin trap 5,5-dimethyl-1-pyrroline *N*-oxide (DMPO) was from Aldrich Chemical Co. (Milwaukee, WI). It was distilled under low pressure before use. Samples were prepared in dry DME or benzene, and reactants were added in the following order: **3d**, spin trap, isoamyl nitrite. Total volumes of the samples were 500 μL. Subsequently the samples were transferred to EPR quartz tubes (internal diameter 5 mm) and gassed with argon for 15 min. Then the tubes were tightly sealed, and EPR spectra were recorded at intervals on the Bruker ER-400 EPR spectrometer operating at 9.5 GHz with 100-kHz field modulation. An aqueous solution of Fremy's salt (0.1 mM in 50 mM K_2CO_3) was used as a standard (separation between the first and second component of the EPR triplet equals 13.1 G). All EPR measurements were performed at room temperature.

Acknowledgment. This work was supported by Grant 1R01 CA21488-10 awarded by the National Cancer Institute, DHHS, to J.W.L. We thank Dr. Tom Nakashima and his associates for the NMR experiments and Dr. Alan Hogg and his colleagues for MS, GCMS, and CIMS spectra. A.M.S. thanks the City University of New York for computer time and for Grant No. 666275.

Registry No. **1**, 137-07-5; **2a**, 77474-06-7; **2b**, 69563-53-7; **2c**, 87028-93-1; **2d**, 117341-22-7; **2e**, 6320-03-2; **2f**, 117341-26-1; **2g**, 117341-27-2; **2h**, 117341-24-9; **2i**, 117341-25-0; **2j**, 117341-28-3; **3a**, 98897-97-3; **3b**, 117341-17-0; **3c**, 117341-18-1; **3d**, 117341-16-9; **4a**, 88571-24-8; **4b**, 117341-21-6; **4c**, 117341-20-5; **4d**, 117341-19-2; **7**, 117341-23-8; **8**, 78726-34-8; **9**, 462-80-6; **10**, 262-20-4; **11**, 259-79-0; **12**, 19061-38-2; **13**, 15254-35-0; DMPO, 3317-61-1; 2-bromothiophenol, 6320-02-1.

Absolute Rate Expressions for the Abstraction of Hydrogen by Primary, Secondary, and Tertiary Alkyl Radicals from Thiophenol[1]

James A. Franz,* Bruce A. Bushaw, and Mikhail S. Alnajjar

Contribution from the Pacific Northwest Laboratory, P. O. Box 999, Richland, Washington 99352. *Received May 5, 1988*

Abstract: Absolute rate expressions for the abstraction of hydrogen from thiophenol in nonane by *tert*-butyl, isopropyl, *n*-butyl, and *n*-octyl radicals were determined by kinetic absorption spectroscopy (KAS). Alkyl radicals were produced by photolysis of dialkyl disulfides or by photolysis of mixtures of di-*tert*-butyl peroxide and trialkylphosphine in the presence of thiophenol. Arrhenium expressions for alkyl radicals from the phosphine method from 255 to 355 K were as follows: *n*-butyl, $\log (k/M^{-1} s^{-1}) = (9.40 \pm 0.13) - (1.74 \pm 0.21)/\theta$, $\theta = 2.303RT$ kcal/mol; isopropyl, $\log (k/M^{-1} s^{-1}) = (9.26 \pm 0.19) - (1.70 \pm 0.21)/\theta$; *tert*-butyl, $\log (k/M^{-1} s^{-1}) = (9.26 \pm 0.26) - (1.50 \pm 0.20)/\theta$. Rate constants at 298 K vary from 0.8×10^8 to 1.5×10^8 $M^{-1} s^{-1}$ for the hydrogen-transfer reactions.

The knowledge of accurate rate expressions for the transfer of hydrogen from thiophenol to alkyl radicals would make available valuable rate standards for the competitive measurement of rapid intramolecular radical reactions. Convenient determination of rate constants of unimolecular radical "clock"[2] reactions such as the cyclopropylmethyl ring opening reaction (eq 1), or the trapping

$$c\text{-}C_3H_5CH_2^{\bullet} \rightarrow CH_2{=}CHCH_2CH_2^{\bullet} \quad (1)$$

$$c\text{-}C_3H_5CH_2^{\bullet} + DH \rightarrow c\text{-}C_3H_5CH_3 + D^{\bullet} \quad (2)$$

$$c\text{-}C_3H_5CH_2^{\bullet} + T \rightarrow c\text{-}C_3H_5CH_2T \quad (3)$$

of kinetic products of readily reversible rearrangements, requires a fast competing hydrogen-transfer (eq 2) or spin-trapping reaction (eq 3). In part because of the lack of accurate rate expressions for fast hydrogen-transfer reactions, rate expressions for spin-trapping reactions were recently measured by optical spectroscopy[3] and radical clock methods[4] for use as fast competitive rate standards. In nonpolar solvents, spin-trapping reactions exhibit bimolecular rate constants (k_3) about an order of magnitude slower than diffusion control.[3,4] Beckwith, Bowry, and Moad[4] have applied new trapping rate expressions to determine the most accurate rate expression to date for the cyclopropylmethyl ring opening reaction, $\log (k_1/s^{-1}) = 13.3 - 7.4/\theta$, over the range 40-130 °C. Mathew and Warkentin[5] reported a rate expression based on estimated competing trapping rates, combined with data from early ESR rate measurements of cyclopropylmethyl rearrangement by Ingold.[6a] While spin-trapping rections are valuable alternatives to hydrogen atom abstraction reactions, the products of trapping reactions usually cannot be analyzed by gas chromatography and are thus somewhat more difficult to quantitate.[4] A need clearly exists for the more simply utilized hydrogen ab-

(1) This work was supported by the Office of Basic Energy Sciences, U.S. Department of Energy, under Contract DE-AC06-76RLO 1830.
(2) Griller, D.; Ingold, K. U. *Acc. Chem. Res.* **1980**, *13*, 317-328.
(3) Chateauneuf, J.; Lustyk, J.; Ingold, K. U. *J. Org. Chem.* **1988**, *53*, 1629-1632.
(4) Beckwith, A. L. J.; Bowry, V. W.; Moad, G. *J. Org. Chem.* **1988**, *53*, 1632-1641.
(5) Mathew, L.; Warkentin, J. *J. Am. Chem. Soc.* **1986**, *108*, 7981-7984.
(6) (a) Maillard, B.; Forrest, D.; Ingold, K. U. *J. Am. Chem. Soc.* **1976**, *98*, 7024. (b) Effio, A.; Griller, D.; Ingold, K. U.; Beckwith, A. L. J.; Serelis, A. K. *J. Am. Chem. Soc.* **1980**, *102*, 1734. The ring closure rate expression is $\log (k_{-1}/s^{-1}) = (10.3 \pm 0.5) - (9.0 \pm 0.5)/\theta$, thus $K = 1.3 \times 10^4$ at 25 °C.

0002-7863/89/1511-0268$01.50/0

Table I. Arrhenius Parameters and Rate Constants[a]

radical	method[b]	log $(A/M^{-1}\ s^{-1})^b$	Ea,[b] kcal/mol	$k(25\ °C)$, $M^{-1}\ s^{-1}$
n-butyl	P	9.41 ± 0.13	1.74 ± 0.21	1.36×10^8
n-octyl	D	9.26 ± 0.13	1.78 ± 0.26	9.2×10^7
isopropyl	P	9.26 ± 0.19	1.70 ± 0.21	1.05×10^8
tert-butyl	P	9.26 ± 0.26	1.50 ± 0.20	1.47×10^8
tert-butyl	D	9.14 ± 0.08	1.69 ± 0.11	8.0×10^7
benzyl	T	8.27 ± 0.14	3.79 ± 0.24	3.13×10^5

[a] Errors are 2σ. [b] Kinetic method: P, photolysis of di-*tert*-butyl peroxide in the presence of trialkylphosphine and PhSH; D, photolysis of dialkyl disulfide; T, competition of termination with abstraction, see ref 10.

straction reactions as fast competition rate standards.

Although thiophenol is known to undergo hydrogen abstraction by alkyl radicals at rates suitable for determining competing radical rearrangements with rate constants in the desired 10^8–10^9 s^{-1} range, no rate expressions and no sufficiently accurate individual rates of reaction of thiophenol with alkyl radicals are available. Reported rate constants for the reaction of alkyl radicals with aryl thiols vary from 1.8×10^8 $M^{-1}\ s^{-1}$ for abstraction of hydrogen from thiophenol by the 2-phenylethyl radical[7] to 4.1×10^9 $M^{-1}\ s^{-1}$ for abstraction of hydrogen by cyclopropyl radical from thiophenol at 298 K.[8] Cyclopentyl radical was reported to abstract hydrogen from naphthalenethiol with a rate constant of 2.1×10^8 $M^{-1}\ s^{-1}$ at 291 K.[9] An absolute rate expression has been determined for the reaction of benzyl radical with thiophenol (Table I).[10] However, no rate expressions for hydrogen transfer from aryl thiols to alkyl radicals have been published. A variety of rather widely scattered rate constants for the reaction of alkyl radicals with simple alkane thiols have been reported.[11]

We report a series of absolute rate expressions for the abstraction of hydrogen from thiophenol by primary, secondary, and tertiary alkyl radicals, determined by kinetic absorption spectroscopy (KAS), which are sufficiently accurate to serve as rate standards for rapid radical rearrangements. The absolute rate data for primary radical abstraction from thiophenol, combined with carefully determined relative rates of the cyclopropylmethyl ring opening versus abstraction of hydrogen from thiophenol,[12] provide a new, accurate expression for the cyclopropylmethyl ring opening reaction with Arrhenius parameters in precise agreement with thermochemical kinetic predictions.

Experimental Section

General Procedures. Nuclear magnetic resonance spectra were obtained with a Varian VXR-300 instrument. Gas chromatography (GC) was carried out by using a Hewlett-Packard Model HP-5890A instrument equipped with capillary inlet system, on-column injection, flame-ionization detection, and a 30-m × 0.25-mm i.d. J.&W. Scientific DB-5 column. Gas chromatography–mass spectrometry (GCMS) was performed with a Hewlett-Packard Model 5890 chromatograph interfaced to a Model 5970 mass selective detector.

Reagents. Tri-*tert*-butylphosphine and tri-*n*-butylphosphine were purchased from Alfa and distilled before use. Triisopropylphosphine was purchased from Alfa and used as received. Nonane was purchased from Aldrich and distilled from $LiAlH_4$ prior to use. Thiophenol was purchased from Aldrich and distilled under argon. Di-*tert*-butyl peroxide was purchased from Aldrich and used as received. Tri-*n*-butylphosphine sulfide was purchased from Alfa. Di-*sec*-butyl disulfide and di-*tert*-butyl disulfide were purchased from Aldrich and carefully distilled before use. Di-*n*-Octyl disulfide[13] ws prepared by dissolving 29.2 g (200 mmol) of octanethiol in 80 mL of 50% aqueous methanol and treating with a methanol solution of iodine until the color of iodine persisted. The reaction mixture was extracted with CH_2Cl_2. The CH_2Cl_2 solution was washed with aqueous sodium thiosulfate to remove excess iodine, dried over $MgSO_4$, concentrated, and distilled (0.01 mmHg, 140–142 °C) to give a yellow oil. The oil was dissolved in pentane, treated with activated charcoal, and passed through a Florisil column to give 22.8 g (79%) of di-*n*-octyl disulfide: ^1H NMR (300 MHz, $CDCl_3$) δ 0.88 (3 H, t), 1.30 (10 H, m), 1.67 (2 H, m), 2.68 (2 H, t); ^{13}C NMR (75.4 MHz, $CDCl_3$) δ 14.41 (2 C), 22.72 (2 C), 28.60 (2 C), 29.28 (6 C), 31.89 (2 C), 39.17 (2 C); GCMS, *m/z* (rel intens) 178 (20), 145 (21), 101 (5), 87 (10), 79 (5), 71 (80), 69 (21), 67 (8), 59 (5), 58 (5), 57 (100), 55 (42).

Determination of the Ratio of S–S to C–S Cleavage in the Photolysis of a Primary Disulfide. GC analysis of a nonane solution containing 5×10^{-2} M di-*n*-octyl disulfide and 1×10^{-2} M PhSH after photolysis at 308 nm (ca. 1000 50-mJ pulses of a 6-mL solution, consuming 2% of the PhSH) revealed a ratio of octane to octanethiol of 1:99. UV–visible spectra of PhSH and di-*n*-octyl disulfide in cyclohexane revealed molar extinction coefficients of 1.4 and 17, respectively, corresponding to optical densities of 1.4×10^{-2} and 8.5×10^{-1}. In the phosphine photolysis experiments below, direct photolysis of thiophenol to produce PhS• at comparable thiophenol concentrations was not detectable, suggesting that contribution of hydrogen atom displacement reactions with di-*n*-octyl disulfide to form octanethiol, leading to a lower apparent yield of C–S cleavage, are insignificant.

Thermal and Photolytic Reactions of Tri-*n*-butylphosphine, Thiophenol, and Diphenyl Disulfide. Thermolysis of AIBN and PhSH in the Presence of Bu_3P. A stock solution was prepared by combining tri-*n*-butylphosphine (0.1 g, 0.25 mM), thiophenol (0.03 g, 0.14 mM), and azobisisobutyronitrile (AIBN) (0.01 g, 0.034 mM) in 2 mL of degassed benzene. An aliquot (200 μL) of the stock solution was micropipeted into 5-mm-i.d. Pyrex tubes. The tubes were freeze-thaw degassed under vacuum, sealed, and then heated at 100 °C for 10 min. GC and GCMS analysis revealed the presence of phenyl dibutyl phosphinothioite ($PhSPBu_2$), its air-oxidized product phenyl dibutyl phosphinothiolate ($PhSP(O)Bu_2$), and tributylphosphine sulfide. Approximately 10% of the starting phosphine was consumed. The ratio ($PhSPBu_2$ + $PhSP(O)Bu_2$)/Bu_3PS was ~1:1. Bu_2PSPh: GCMS, *m/z* (rel intens) 254 (20, M^+), 225 (50), 212 (14), 197 (10), 183 (23), 170 (100), 169 (21), 156 (40), 141 (46), 140 (13), 94 (30), 92 (70), 91 (60), 77 (55), 63 (27), 57 (13), 55 (13); $Bu_2P(O)SPh$: GCMS, *m/z* (rel intens) 270 (28, M^+), 241 (28), 214 (36), 193 (12), 186 (57), 161 (75), 158 (66), 157 (28), 135 (15), 110 (30), 109 (28), 92 (37), 77 (18), 65 (24), 62 (100), 57 (15). Tributylphosphine sulfide: GCMS, *m/z* (rel intens) 234 (23, M^+), 178 (25), 177 (6), 123 (7), 122 (100), 87 (14), 80 (14), 79 (6), 65 (6), 63 (7), 57 (20), 55 (12).

Photolysis of AIBN/PhSH or PhSSPh in the Presence of Bu_3P. In a separate experiment, stock solutions consisting of tri-*n*-butylphosphine, PhSH, and AIBN at the same concentrations as above, or of tri-*n*-butylphosphine (0.1 g, 0.25 mM), and diphenyl disulfide (0.06 M) in 2 mL of degassed benzene were prepared. Photolysis of the solutions (450-W medium-pressure Hg/Xe lamp) for 15 min at room temperature, followed by exposure to air, resulted in 5–7% consumption of Bu_3P and gave $PhSPBu_2$, $PhSP(O)Bu_2$, and Bu_3PS with identical GC retention times and mass spectra of the products produced in the thermal reaction of Bu_3P, AIBN, and PhSH above. The average ratio ($PhSPBu_2$ + $PhSP(O)Bu_2$)/Bu_3PS in the photolysis experiments was 4.5:1.

Thermal Decomposition of Bu_3P and PhSSPh. A mixture of PhSSPh and Bu_3P in C_6D_6 revealed no formation of $PhSBu_2$ or Bu_3PS after 2 h at room temperature. Thermal decomposition of PhSSPh (0.06 M) and Bu_3P (0.25 M) at 100 °C for 6 min in benzene gave predominately Bu_2PS and $Bu_2P(O)SPh$, and a small yield of Bu_3PS, in a ratio (Bu_2PS + $Bu_2P(O)SPh$)/Bu_3PS of >150:1. Approximately 7–10% of the starting phosphine was consumed. Upon discovery that butylphenyl sulfide coeluted with Bu_3P during GC analysis, the experiment was repeated using an excess of PhSSPh (6.65 mmol) over Bu_3P (4.0 mmol), which results in entrainment of unreacted Bu_3P apparently as the phosphorane, which does not elute from the GC column, permitting the analysis of BuSPh, which gave a mass spectrum identical to that of authentic material: *m/z* (rel intens) 166 (43, M^+), 123 (24), 111 (10), 110 (100), 109 (19), 77 (10), 66 (9), 65 (12), 51 (12). The experiment was repeated with the addition of α-methylstyrene (0.2 mmol) as a radical inhibitor. The ratio of ($PhSPBu_2$ + $PhSP(O)Bu_2$)/Bu_3PS remained unchanged at >150:1.

Methods of Radical Production. A. Photolysis of Di-*tert*-butyl Peroxide in the Presence of Trialkylphosphines and PhSH. Alkyl radicals were produced by 308-nm excimer laser pulse photolysis of thermostated

(7) Russell, G. A.; Tashtoush, H. *J. Am. Chem. Soc.* **1983**, *105*, 1398–1399.
(8) Johnston, L. J.; Scaiano, J. C.; Ingold, K. U. *J. Am. Chem. Soc.* **1984**, *106*, 4877–4881.
(9) Smaller, B.; Remko, J. R.; Avery, E. C. *J. Chem. Phys.* **1968**, *48*, 5174–5181.
(10) Franz, J. A.; Suleman, N. K.; Alnajjar, M. S. *J. Org. Chem.* **1986**, *51*, 19–25.
(11) Encinas, M. V.; Wagner, P. J.; Scaiano, J. C. *J. Am. Chem. Soc.* **1980**, *102*, 1357–1360.
(12) Newcomb and Glenn report a relative rate expression for reaction of the cyclopropylmethyl radical with thiophenol in tetrahydrofuran vs ring opening; $\log (k_i/k_6) = (3.6 \pm 0.14) - (5.1 \pm 0.2)/\theta$ (errors are 2σ): Newcomb, N.; Glenn, A. G. *J. Am. Chem. Soc.*, following paper in this issue.
(13) McMillan, F. H.; King, J. A. *J. Am. Chem. Soc.* **1948**, *70*, 4143–4150. Westlake, H. E.; Dougherty, G. *J. Am. Chem. Soc.* **1942**, *64*, 149.

solutions of di-*tert*-butyl peroxide in the presence of trialkylphosphines[14] and thiophenol. Solutions consisted of 0.2–0.3 M trialkylphosphine, 0.1–0.2 M di-*tert*-butyl peroxide, and from 5×10^{-3} to 1.2×10^{-2} M PhSH in nonane.

B. Photolysis of Disulfides in the Presence of Thiophenol. Solutions containing 0.01–0.03 M di-*n*-octyl or di-*tert*-butyl disulfide and $(1–1.3) \times 10^{-2}$ M thiophenol were irradiated at 308 nm to produce the corresponding alkyl radical.

Concentration-Dependence Test of Pseudo-First-Order Kinetic Behavior. To determine if the observed rate of reaction of alkyl radicals involves a contribution from competing first-order or pseudo-first-order processes k_0, resulting in an apparent rate of abstraction given by $\text{rate}_{obsd} = k_0 + k_6[\text{PhSH}]$, the reaction of isopropyl radical, produced from triisopropylphosphine and di-*tert*-butyl peroxide, with thiophenol was determined over a range of thiophenol concentrations from 1.3×10^{-3} M to 2.8×10^{-2} M. A plot of observed rate vs [PhSH] gave a linear plot ($r^2 = 0.995$) with a slope of $(9.1 \pm 0.5) \times 10^7$ M^{-1} s^{-1} and a near-zero intercept of $(-1.02 \pm 11) \times 10^4$ M s^{-1}. Variation of PhSH concentration also had no effect on the observed rate of reaction of the *tert*-butyl radical, indicating that, by contrast with reactions of alkyl radicals with Bu_3SnH,[14] competing first-order and pseudo-first-order processes k_0 are negligible for PhSH. Thus, PhSH concentrations were not varied for butyl and octyl radical reactions.

Determination of UV–Visible Spectra during the Reaction of *n*-Butyl Radical with Thiophenol. UV–visible spectra from 350 to 650 nm were recorded for time delays of 50 ns–3.5 μs following the excimer laser pulse during the reaction of *n*-butyl radical with thiophenol. Three bands centered around 380, 440, and 490 nm were observed. The spectra were unchanged throughout the course of the reaction and were identical to a published[15] spectrum of thiophenoxyl radical. For comparison, a spectrum of thiophenoxyl radical was obtained by photolysis of diphenyl disulfide in nonane. Photolysis of diphenyl disulfide at 10^{-3} M produced the same three bands, but with a more intense central band around 440 nm, probably attributable to $(PhS)_2S^{\bullet}Ph$.[15,16] At a diphenyl disulfide concentration of less than 10^{-4} M, the spectra determined between 350 and 550 nm were identical to spectra taken during the reaction of butyl radical with thiophenol.

Kinetic Absorption Spectrometer System. Sample Cell. The sample cell consisted of a $6 \times 1 \times 1$ cm (length × width × height) rectangular photolysis chamber equipped with a transfer tube, high-vacuum valves, and sample reservoir to allow freeze–thaw degassing of the solution and inert transfer of the solution to the photolysis chamber. Detection was accomplished through the 6-cm dimension, with the excimer pulse perpendicular to the probe beam axis. Of the 6-cm dimension, 2.5 cm was irradiated with the excimer laser. The cell was mounted in an insulated chamber with temperature controlled (−30 to 90 ± 1 °C) by a thermostated stream of nitrogen.

Spectrometer System. The cell was irradiated with a pulsed excimer laser (308 nm, Lambda-Physik EMG 53), with continuous wave (cw) detection provided by a Coherent I-18 Ar ion laser operated at 476 nm. The excimer laser was defocused to maintain energy densities less than ~10 mJ/cm^2-pulse to reduce acoustic wave deflection of the detection laser. The detection beam was passed through a 0.125-m Oriel monochromator to discriminate against fluorescence and scattered 308-nm light. The transient transmission signal was recorded by digitizing (Gould-Biomation 8100) the voltage from an RCA 6199 or Hamamatsu R1509 photomultiplier tube (PMT) at the exit of the monochromator. Variable-wavelength detection was also possible with a Kratos 1000-W short arc lamp power supply interfaced with a PRA Model M305 lamp pulser network.

Since observed transmission changes are typically only 1–2% of the detected signal amplitude, recording data of sufficient quality for kinetic analysis requires noise to be ≤0.1% of the signal amplitude on a submicrosecond time scale. To reduce photon statistical noise, the Ar detection laser was operated at ca. 100-mW output power. The PMT was modified to operate with the first five of eight dynodes, retaining time response without saturation. The PMT was mounted in an electromagnetically shielded housing with an integrally shielded dc 50-MHz preamplifier (Pacific Instruments 3262RF/2A44) and was close-coupled to the digitizer. The effective dynamic range of the digitizer (8 bit) is increased by measuring the dc PMT voltage just prior to the photolysis pulse, then switching to ac signal coupling, and increasing sensitivity by a factor of 100 during photolysis and the subsequent reaction period, measuring the change in transmission. The raw voltages are converted to absorbance values according to $A = \log [I_0/(I_0 - I)] = \log [V/(V - V_{ac}/100)]$. A computer (DEC PDP 11/03) reads raw data from the digitizer and controls its gain, coupling, and speed. The computer also controls synchronization of the photolysis laser and a shutter on the detection laser. The foreground (experimental) signal is corrected for fluorescence, excimer laser scatter, rf noise, and zero level offset by subtracting the signal produced by photolysis of the sample with the Ar detection laser blocked. Signal averaging could be performed, but was limited (typically 10 laser shots) to prevent the buildup of photoproducts.

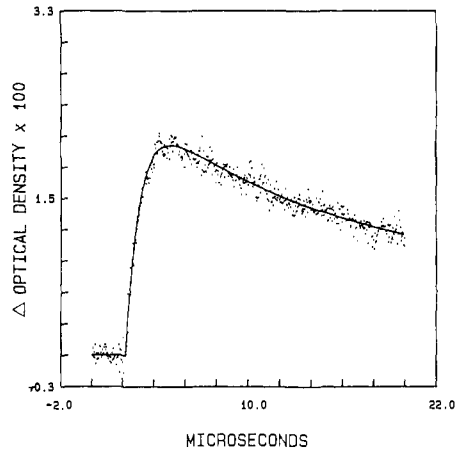

Figure 1. Absorbance curve for the reaction of *tert*-butyl radical with thiophenol (7.8×10^{-3} M) with detection at 476 nm. The solid line was generated by numerical integration of eq 11 and 12 using $k_7 = 3.2 \times 10^9$ M^{-1} s^{-1}, $k_8 = 2.95 \times 10^9$ M^{-1} s^{-1}, and $k_9 = 2.7 \times 10^9$ M^{-1} s^{-1} (ref 27), $k_6 = 1.354 \times 10^8$ M^{-1} s^{-1}, an initial alkyl radical concentration, [R•(0)], of 1.21×10^{-5} M, and $\epsilon l = 2.015 \times 10^3$/M, where ϵ is the molar extinction coefficient (M^{-1} cm^{-1}) and l is the irradiated path length traversed by the detection beam (2.5 cm). [R•(∞)], k_6, and ϵl were determined by a fit of the experimental data using the Simplex algorithm (ref 28), using estimates of k_7, k_8, and k_9 define a unique set of values [R•(0)], k_6, and ϵl.

Diode Array Spectrometer. The spectrometer system consisted of a Tracor-Northern Model TN-1710A multichannel analyzer interfaced to a Model TN-6048-3 512-element holographic grating diode array detector, which was interfaced to the kinetic absorption spectroscopy system described above, with substitution of the cw Ar ion laser with a 1000-W, high-pressure, xenon arc lamp. The spectrometer was gated on for periods of 20–100 ns after variable delay times of 50 ns or greater after the excimer pulse. Absorption spectra were obtained by dividing a spectrum taken following an excimer pulse by the spectrum with no excitation pulse. Spectra were obtained from 350 to 650 nm.

Treatment of Kinetic Data. Raw transmittance data were converted to absorbance by the relation $A(t) = \log_{10} (I_0/I(t))$. For kinetic data collected from experiments with initial radical concentrations greater than ~10^{-6} M, and observed rates of hydrogen abstraction of ~1×10^6 M/s, direct pseudo-first-order analysis of the rise portion using the maximum of the curve (Figure 1) as $A(\infty)$ will give a rate constant that is consistently higher than the actual rate, due to radical termination events occurring to various extents during the rise period. An improved estimate of $A(\infty)$, which eliminates most of the error in rate constant, was obtained as follows: Using the decay portion of the absorbance curve, least-squares treatment of $1/A(t)$ vs t provides the absorbance terminate rate constant, $2k_9/l\epsilon$. The absorbance change due to self-termination during the time increment Δt of each data point is $(2k_9/l\epsilon)(A(t))^2\Delta t$. Starting from the excitation pulse, the running total, $\sum(2k_9/l\epsilon)(A(t))^2\Delta t$, is added to each data point of the raw absorbance curve, Figure 1, resulting in the termination-corrected curve, Figure 2. The plateau region of the termination-corrected absorbance curve is taken as $A(\infty)$ to calculate the experimental pseudo-first-order abstraction rate constant (k_{obsd}) from a least-squares treatment of ln $(A(\infty) - A(t))$ vs time of the initial rise portion of the curve. Using the maximum of this curve as $A(\infty)$ eliminates most (75%; see Table II and discussion below) of the rate constant error due to the incursion of alkyl–alkyl, alkyl–thiophenoxyl, and thiophenoxyl–thiophenoxyl termination during the rise portion of the curve.

Concentrations of the donor, [PhSH], were corrected for changes in density using the temperature coefficient of expansion for nonane.[17]

(14) Chatgilialoglu, C.; Ingold, K. U.; Scaiano, J. C. *J. Am. Chem. Soc.* **1987**, *103*, 7739–7742.
(15) Thyrion, F. C. *J. Phys. Chem.* **1973**, *77*, 1478–1482.
(16) Burkey, T. J.; Griller, J. *J. Am. Chem. Soc.* **1985**, *107*, 246–249.

(17) The method of Gunn and Yamada was used to estimate the temperature dependence of density of nonane: Reid, R. C.; Pruassnitz, J. M.; Sherwood, T. K. *The Properties of Gases and Liquids*, 3rd ed.; McGraw-Hill: New York, 1977; pp 60–61.

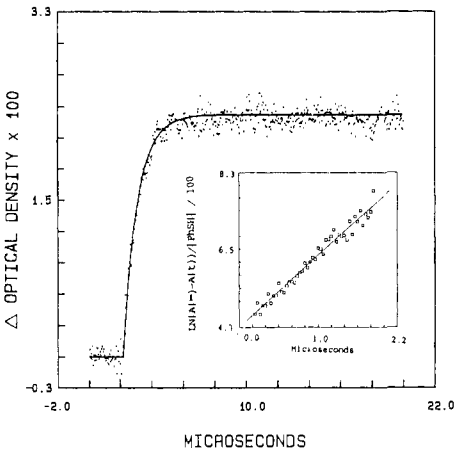

Figure 2. Plot of termination-corrected data of Figure 1. A second-order fit of the decay portion of Figure 1 yields $2k_9/l\epsilon = 1.32 \times 10^6$. Addition of a running total of $\sum(2k_9/l\epsilon)A(t)^2\Delta t$ to each data point of Figure 1 yields the corrected experimental points. Performing a pseudo-first-order fit of the rise portion (inset) yields $k_6 = (1.37 \pm 0.04) \times 10^8$ M^{-1} s^{-1}, compared to 1.83×10^8 M^{-1} s^{-1} from pseudo-first-order treatment of the uncorrected curve. The solid line is the corrected curve predicted from numerical integration using values of $k_6 = 1.35 \times 10^8$ M^{-1} s^{-1}, initial radical concentration = 1.21×10^{-5} M, and $2k_9/l\epsilon = 1.34 \times 10^{-6}$ determined from a Simplex fit of Figure 1 with termination constants fixed at values cited in Table III.

Results and Discussion

Arrhenius expressions and rate constants are provided in Table I for reactions of primary, secondary, tertiary, and benzyl[10] radical with thiophenol. Figure 1 depicts a typical example of raw absorbance data, and Figure 2 shows the result of application of the termination correction procedure. The inset of Figure 2 shows the pseudo-first-order treatment of the rise portion of the termination-corrected data. Figure 3 provides an Arrhenius plot for the reaction of *tert*-butyl radical with thiophenol.

Mechanisms of Formation and Reactions of Alkyl and Thiophenoxyl Radicals. A. Production of Radicals from Phosphines. The production of alkyl radicals by the photolysis of di-*tert*-butyl peroxide in the presence of phosphines (eq 4, 5) has been described

$$t\text{-BuOOBu-}t \xrightarrow{h\nu,\ 308\ \text{nm}} 2\ t\text{-BuO}^\bullet \quad (4)$$

$$t\text{-BuO}^\bullet + R_3P \rightarrow [t\text{-BuOP}(^\bullet)R_2] \rightarrow t\text{-BuOPR}_2 + R^\bullet \quad (5)$$

$$R^\bullet + PhSH \rightarrow RH + PhS^\bullet \quad (6)$$

$$2R^\bullet \rightarrow R_2 + RH + (R(-H)) \quad (7)$$

$$R^\bullet + PhS^\bullet \rightarrow PhSR \quad (8)$$

$$2PhS^\bullet \rightarrow PhSSPh \quad (9)$$

by Chatgilialglu et al.[14] Equations 4–9 describe the pathways of formation and decay of radicals. Production of alkyl radicals is complete within 40 ns (5 half-lives of formation and α-scission of the phosphoranyl radical[14]) of the excimer laser pulse at phosphine concentrations (0.2–0.3 M) employed in the photolysis experiments. The alkyl radicals are mostly consumed in the abstraction reaction (eq 6), with small contributions from self- (eq 7) and cross-termination (eq 8). The thiophenoxyl radical decays almost entirely by self-termination (eq 9), with a small contribution from cross-termination. Predicted reaction channels of the alkyl radicals are presented in Table II.

A possible additional reaction of the thiophenoxyl radical is addition to trialkylphosphine:

$$PhS^\bullet + R_3P \rightarrow PhSP(^\bullet)R_3 \quad (10)$$

An estimate[18] of the rate constant for addition of butanethiyl radical to tributylphosphine, 1.5×10^9 M^{-1} s^{-1}, has been reported, and Burkey et al.[19] reported a preliminary rate constant of ca. 10^6 M^{-1} s^{-1} for addition of thiophenoxyl radical to tributylphosphine. Thus, it was important to determine whether the thiophenoxyl radical was being diverted during the initial rise time to form an intermediate phosphoranyl radical with a different extinction coefficient at 476 nm (eq 10) or a changing absorbance due to unimolecular decomposition of the phosphoranyl radical, resulting in an erroneous value of k_6. Thus, UV–visible spectra (350–650 nm) were determined in reactions of *n*-butyl radical with thiophenol, with delays of between 50 and 3500 ns following the excimer pulse. The spectra remained unchanged over time except for a decrease in signal intensity as termination progressed. The observed spectra were identical to the spectrum of the thiophenoxyl radical, which suggests that addition (k_{10}) is slow relative to self-termination or is readily reversible, with the equilibrium favoring the left side of eq 10. The thermochemistry for addition/β-scission (vide infra) predicts an irreversible addition/β-scission step, although the reliability of the thermochemical data is probably inadequate to strictly rule out reversibility.[20] The

Table II. Predicted Rate Errors as a Function of Initial Radical Concentration Using the Termination Correction Method[a]

	t-Bu$^\bullet$ Rxn Pathway,[c] %			$k_6/10^8$ M^{-1} s^{-1}		
[*t*-Bu$^\bullet$(0)][b]	abstr (k_6)	self-term (k_7)	cross-term (k_8)	model	corr[d] (% error)	uncorr[e] (% error)
1.0×10^{-6}	99.6	0.3	0.1	1.33	1.34 (0.3)	1.39 (4.5)
5.0×10^{-6}	97.8	1.5	0.7	1.33	1.36 (2.3)	1.54 (15.8)
1.0×10^{-5}	95.8	2.9	1.3	1.33	1.39 (4.5)	1.68 (26.3)
2.5×10^{-5}	90.4	6.9	2.7	1.33	1.48 (11.3)	2.05 (54.1)
5.0×10^{-5}	83.2	12.4	4.3	1.33	1.60 (20.3)	2.56 (92.5)
Error and Rxn Pathway Estimates for Data of Figure 1[f]						
1.21×10^{-5}	95.1	3.4	1.5	1.354	1.43 (4.3)	1.77 (33.1)
experiment					1.37 ± 0.04	1.83 ± 0.04

$k_9/l\epsilon = 1.32 \times 10^6$ (expt)
$k_9/l\epsilon = 1.34 \times 10^6$ (Simplex fit)
$l\epsilon = 2.0152 \times 10^3$ (Simplex fit)
$l = 2.5$ cm, $\epsilon = 806$ M^{-1} cm^{-1}

[a] From numerical integration of eq 10 and 11 using a PhSH concentration of 7.8×10^{-3} M, a model abstraction rate constant $k_6 = 1.33 \times 10^8$ M^{-1} s^{-1}, and termination rate constants $k_7 = 3.2 \times 10^9$ M^{-1} s^{-1}, $k_8 = 2.975 \times 10^9$ M^{-1} s^{-1}, and $k_9 = 2.7 \times 10^9$ M^{-1} s^{-1}. [b] Initial radical concentration. [c] Percent of *tert*-butyl radicals consumed in abstraction, self-termination, and cross-termination. [d] Corrected rate constant k_6 determined from a pseudo-first-order treatment of the rise portion of the theoretical termination-corrected curve. Values in parentheses are the percent errors. [e] Uncorrected rate constant k_6 determined from a pseudo-first-order treatment of the rise portion of the theoretical uncorrected curve. Values in parentheses are the percent errors. [f] The rate constant $k_6 = 1.35 \times 10^8$ M^{-1} s^{-1}, and initial radical concentrations were determined by Simplex fit of Figure 1 data using termination constants fixed at the values of footnote *a*, above. [R$^\bullet$(0)] and k_6 from the fit were then used to predict the *apparent* value of k_6 with and without termination correction and associated errors.

(18) (a) Walling, C.; Basedow, O. H.; Savas, S. *J. Am. Chem. Soc.* **1960**, *82*, 2181–2184. (b) Walling, C.; Pearson, M. S. *J. Am. Chem. Soc.* **1964**, *86*, 2262–2266.

(19) Burkey, T. J.; Hawari, J. A.; Lossing, F. P.; Lusztyk, J.; Sutcliffe, R.; Griller, D. *J. Org. Chem.* **1985**, *50*, 4966–4967, and references therein.

(20) (a) Benson, S. W. *Thermochemical Kinetics. Methods for the Estimation of Thermochemical Data and Rate Parameters*, 2nd ed.; Wiley: New York, 1976. (b) The P=S bond strength is 91.5 kcal/mol: Hartley, S. B.; Holmes, W. S.; Jacques, J. K.; Mole, M. F.; McCoubrey, J. C. *Q. Rev., Chem. Soc.* **1963**, *17*, 204. The SH bond strength is 89 kcal/mol: Braumann, J. I. In *Frontiers in Free Radical Chemistry*; Pryor, W. A., Ed.; Academic Press: New York, NY, 1980; pp 23–30, and references therein. The heat of formation of phenyl radical is 78.5 kcal/mol: Rodgers, A. S.; Golden, D. M.; Benson, S. W. *J. Am. Chem. Soc.* **1967**, *89*, 4578. The heat of formation of PhS$^\bullet$ was taken from: Colussi, A. J.; Benson, S. W. *Int. J. Chem. Kinet.* **1977**, *9*, 295. Other thermochemical values were taken from: Cox, J. D.; Pilcher, G. *Thermochemistry of Organic & Organometallic Compounds*: Academic: New York, 1970.

(21) Brown, D. H.; Cross, R. J.; Millington, D. *Inorg. Nucl. Chem. Lett.* **1975**, *11*, 783; *J. Chem. Soc., Dalton Trans.* **1976**, 334

relative rate of termination (eq 9) to addition (eq 10) is given by $2k_9[PhS^\bullet]^2/k_{10}[PhS^\bullet][PBu_3]$. With a self-termination rate constant for thiophenoxyl, k_9, of 2.7×10^9 M^{-1} s^{-1}, $[PBu_3] = 0.2$–0.3 M, and thiophenoxyl concentrations between 10^{-6} and 10^{-5} M, the relative rate of termination to addition will be greater than 10:1 only if k_{10} lie between 10^3 and 10^4 M^{-1} s^{-1} or less, which is 2–3 orders of magnitude lower than the value of Burkey et al.[19]

The slow apparent rate of rection of thiophenoxyl radical with trialkylphosphines is consistent with the failure of thiophenol to under a radical chain reaction with either trialkyl phosphites or -phosphines, while alkane thiols react in an efficient chain with both phosphites and phosphines.[18] Analysis of the thermochemistry for thiophenoxyl radical reaction with tributylphosphine reveals a nearly thermoneutral initial addition/β-scission step, compared to the highly exergonic addition/β-scission of butanethiyl radical:[20]

Thiophenoxyl

$\Delta H^\circ_{f,298}$ 56.8 −60.2 78.5 −85.0
$PhS^\bullet + PBu_3 \rightarrow Ph^\bullet + SPBu_3$ $\Delta H^\circ = -3.1$ kcal/mol

$\Delta H^\circ_{f,298}$ 78.5 26.94 56.8 19.8
$Ph^\bullet + PhSH \rightarrow PhS^\bullet + PhH$ $\Delta H^\circ = -28.8$ kcal/mol

$PhSH + PBu_3 \rightarrow SPBu_3 + PhH$ $\Delta H^\circ = -31.9$ kcal/mol

Butanethiyl

$\Delta H^\circ_{f,298}$ 15.9 −60.2 17.7 −85.0
$BuS^\bullet + PBu_3 \rightarrow Bu^\bullet + SPBu_3$ $\Delta H^\circ = -23.0$ kcal/mol

$\Delta H^\circ_{f,298}$ 17.7 −21.0 −30.2 15.9
$Bu^\bullet + BuSH \rightarrow BuH + BuS^\bullet$ $\Delta H^\circ = -11.0$ kcal/mol

$BuSH + PBu_3 \rightarrow BuH + SPBu_3$ $\Delta H^\circ = -34.0$ kcal/mol

A comparable thermochemical analysis cannot be performed for α-scission, because of the lack of suitable thermochemical data. However, experiments in which PBu_3 was exposed to thermal and photolysis sources of $PhS^\bullet$ revealed that α-scission of a butyl radical from the phosphoranyl radical intermediate occurs competitively with β-scission, with k_β/k_α varying from 1:1 to 5:1:

$$PhSP(^\bullet)Bu_3 \rightarrow PhSPBu_2 + Bu^\bullet \quad (11)$$

At elevated temperatures (100 °C), an ionic reaction of the phosphonium salt from PhSSPh and PBu_3 contributes to the formation of phenyl dibutyl phosphinothioite ($PhSPBu_2$) and BuSPh in equimolar amounts:[25]

$$PhSPBu_3^+ {}^-SPh \rightarrow PhSPBu_2 + BuSPh \quad (12)$$

Thus both α- and β-scission processes appear to be approximately thermoneutral. We conclude that either the addition of $PhS^\bullet$ is much slower than the reported estimate[19] or the addition reaction is readily reversible. The reversibility of addition of alkanethiyl radicals to phosphines has been reported.[21] Few examples of ESR or optical spectra of thiophosphoranyl[22,23] radicals have been published, and further work to characterize the thermochemistry and unimolecular lifetimes of thiophosphoranyl radicals such as $PhSP(^\bullet)Bu_3$ is needed.

Finally, diphenyl disulfide, formed as the initial termination product, does not accumulate in the phosphine kinetic experiments and, when present in the thiophenol, is consumed by the *tert*-butyl peroxide–trialkylphosphine reaction medium, as evidenced by the convenient lack of a prompt absorption in the kinetic experiments (diphenyl sulfide is usually present at 0.1–0.3% of thiophenol, and a fast rise was usually observed in kinetic experiments using dialkyl disulfides from direct photolysis of PhSSPh). The lack of an instantaneous absorbance following the excimer laser pulse in the phosphine experiments reveals that PhSH is not photolyzed directly to produce $PhS^\bullet$ in significant amounts. Although PhSSPh[24] is subject to facile radical displacement reactions, the main pathway of consumption of PhSSPh is described by eq 13:[25]

$$Bu_3P + PhSSPh \rightarrow Bu_3P(SPh)_2 + H_2O \rightarrow Bu_3PO + 2PhSH \quad (13)$$

In summary, the kinetic scheme for the phosphine method is described by eq 4–9 with regeneration of thiophenol via eq 13 and negligible contribution from the addition pathway of eq 10.

B. Production of Alkyl Radicals from the Photolysis of Disulfides. Photolysis of dialkyl disulfides produced adequate concentrations of alkyl radicals via C–S cleavage to permit their use as radical sources. Primary dialkyl disulfides undergo 1% C–S cleavage and 99% S–S cleavage. Tertiary disulfides were qualitatively observed to undergo more efficient C–S cleavage, from the higher thiophenoxyl product signals observed in kinetic experiments.

Potential sources of interference with detection of the thiophenoxyl radical in the disulfide experiments (eq 14, 15) are direct

$$RSSR \xrightarrow{305\ nm} 2RS^\bullet \quad (14)$$

$$RSSR \xrightarrow{308\ nm} RSS^\bullet + R^\bullet \quad (15)$$

abstraction of hydrogen from thiophenol by an alkanethiyl radical, interference by absorption by the alkane perthiyl radical, and formation of sulfuranyl radicals with absorbance at 476 nm. The UV–visible spectrum from photolysis of the disulfides in the absence of PhSH produced no absorption above 350 nm, and thus the primary photoproducts $RS^\bullet$ and $R^\bullet$ did not interfere with detection of $PhS^\bullet$. Since abstraction of hydrogen by $RS^\bullet$ from thiophenol is 3 orders of magnitude slower than hydrogen transfer to alkyl radicals,[26] abstraction by $RS^\bullet$ of hydrogen from thiophenol is negligible on the time scale of reaction of the alkyl radical with thiophenol. Possible inteference by the absorption of the perthiyl radical ($RSS^\bullet$) or sulfuranyl ($RS_2S(^\bullet)R$) radicals with detection at 476 nm was ruled out by obtaining UV–visible spectra following the photolysis of di-*n*-octyl disulfide in the absence of PhSH. The resulting spectra were similar to that reported for *tert*-butylthiyl[19] radical, exhibiting an absorbance maximum at 375 nm and negligible absorption at 476 nm in the absence of PhSH.

For the disulfide experiments, termination of both the alkyl radical and the product thiophenoxyl radical will occur with the dominant alkanethiyl radical (eq 16, 17). Thus, the disulfide

$$RS^\bullet + R^\bullet \rightarrow RSR \quad (16)$$

$$RS^\bullet + PhS^\bullet \rightarrow RSSPh \quad (17)$$

experiments were carried out with lower initial radical concentrations and weaker product radical signals in order to avoid excessive cross-termination (eq 17) during the rise portion of the kinetic experiment. Consequently, while the 30–40% lower observed rates (probably due to some interference from early cross-termination) from the disulfide experiments are in satisfactory agreement with the phosphine experiments (Table I), we recommen the phosphine results for use as rate standards.

Analysis of Kinetic Data. For both phosphine and disulfide methods, the time dependence of alkyl and product thiophenoxyl radicals is given by eq 18 and 19. If the initial alkyl radical

(22) Davies, A. G.; Griller, D.; Robert, B. P. *J. Organomet. Chem.* **1972**, *38*, C8–C10.

(23) (a) Bentrude, W. G. In *Free Radicals*; Kochi, J. K., Ed.; Wiley: New York, 1973; Vol. II, pp 595–663. (b) Roberts, B. P. In *Advances in Free Radical Chemistry*; Vol. 6, Williams, G. H., Ed.; Heyden: London, 1980; pp 225–289.

(24) Bentrude, W. G.; Kawashima, T.; Keys, B. .; Garrossian, M.; Heide, W.; Wedegaertner, D. A. *J. Am. Chem. Soc.* **1987**, *109*, 1227–1235.

(25) (a) Formation of organophosphorus thio esters from disulfides and phosphines: Grayson, M.; Farley, C. E. *J. Org. Chem.* **1967**, *32*, 236. (b) Dehydration reactions of Bu_3P/PhSSPh: Barton, D. H. R.; Motherwell, W. B.; Simon, E. S.; Zard, S. Z. *J. Chem. Soc., Chem. Commun.* **1984**, 337, and references therein. (c) Reactivity of phosphorus nucleophiles and an exhaustive review of related chemistry: Overman, L. E.; Matzinger, D.; O'Connor, E. M.; Overman, J. D. *J. Am. Chem. Soc.* **1974**, *96*, 6081.

(26) Octanethiyl radical abstracts hydrogen from thiophenol with a rate constant of 1.4×10^5 M^{-1} s^{-1} at 298 K in nonane: Alnajjar, M. S.; Garrossian, M.; Franz, J. A., unpublished results.

$$d[R^\bullet]/dt = -k_6[R^\bullet][PhSH] - 2k_7[R^\bullet]^2 - k_8[R^\bullet][PhS^\bullet] \quad (18)$$

$$d[PhS^\bullet]/dt = k_6[R^\bullet][PhSH] - k_8[R^\bullet][PhS^\bullet] - 2k_9[PhS^\bullet]^2 \quad (19)$$

$$d[PhS^\bullet]/dt = k_6[R^\bullet][PhSH] = k_6(PhS^\bullet(\infty) - PhS^\bullet(t))[PhSH] \quad (20)$$

$$-\ln [(A_\infty - A(t))/A_\infty] = k_6[PhSH]t \quad (21)$$

concentration is sufficiently low, the last two terms in eq 18 and 19 will be insignificant, and $[R^\bullet(0)] = [PhS^\bullet(\infty)]$, leading to eq 20. Integration of eq 20 and conversion to absorbance provides eq 21. For typical rates of abstraction observed in the kinetic experiments, 10^6 M s^{-1}, and radical termination rate constants from 1×10^9 to 10^9 M^{-1} s^{-1}, the last two terms of eq 18 only become insignificant (less than 5% error in abstraction rate constant) below initial alkyl radical concentrations of $\sim 5 \times 10^{-6}$ M. Thus, a method of correction for early termination was necessary to obtain accurate rate constants, and the procedure described in the Experimental Section above was applied throughout. The termination correction restores the decay in the raw absorbance curve (Figure I) due to self-termination of thiophenoxyl. The plateau region of the corrected absorbance curves gives an improved value of $A(\infty)$ for use in the pseudo-first-order fit (eq 21) of the corrected absorbance curve (Figure II).

Analysis of Errors from the Termination Correction Method. The error in measured rate constant from application of the termination correction was estimated as a function of initial radical concentration by numerical integration of eq 18 and 19. Pseudo-first-order treatment (log $(C(\max) - C(t))$ vs time) of the rise portion of the numerically generated, uncorrected concentration curve provides the theoretical value of k_6, uncorrected.

Performing a correction of the numerically generated concentration curve by adding a running total, $\sum 2k_9C(t)^2\Delta t$, where Δt is the length of the increment, to each increment point, provides the theoretical termination-corrected curve. Pseudo-first-order analysis of the rise portion of the corrected theoretical curve provides the theoretical corrected rate constant k_6. The results of this exercise are shown in Table II for an observed rate near 1×10^6 M s^{-1} (the typical observed reaction rate), using accurate termination rate constants available for the *tert*-butyl radical and thiophenoxyl termination constants estimated from the Smoluchowski equation (eq 22).[16] As shown in Table II, for alkyl radicals with ordinary termination constants ($(2-3) \times 10^9$ M^{-1} s^{-1}), a pseudo-first-order treatment using the maximum of the uncorrected curve will lead to a +30% error in rate constant, which can be reduced to ~5% by the termination-correction method. Application of the termination correction reduces the systematic error to well within errors from other sources.

Estimation of the Molar Extinction Coefficient of the Thiophenoxyl Radical and Initial Alkyl Radical Concentrations. The initial alkyl radical concentration and the extinction coefficient of thiophenoxyl radical can be extracted from the experimental absorbance curve if independent assignment of the extinction coefficient of PhS• or independent assignment of the termination constants k_7, k_8, and k_9 can be made. By use of the Simplex curve-fitting procedure described below, a reliable estimate of the amount of alkyl radical lost in self- and cross-termination can be estimated, providing an accurate verification of the magnitude of errors in the abstraction rate constant k_6. An estimate of k_9 was obtained by use of the Smoluchowski equation:

$$2k_9 = (8 \times 10^{-3})\sigma\pi D_{AB}N \quad (22)$$

The predicted diffusion coefficient for the model of thiophenoxyl radical, thiophenol, is 2.43×10^{-5} cm^2 s^{-1} in nonane, and $2k_g = 5.48 \times 10^9$ M^{-1} s^{-1} at 298 K. The *tert*-butyl self-termination constant k_7 in nonane was taken as the average of octane and decane values,[27a] and the cross-termination rate k_8 was taken as the average of the two symmetric termination rates k_7 and k_9. Having assigned the termination constants, the abstraction rate constant k_6, the initial radical concentration $[R^\bullet(0)]$, and the molar extinction coefficient ϵ are uniquely defined and can be extracted from the experimental absorbance curve.

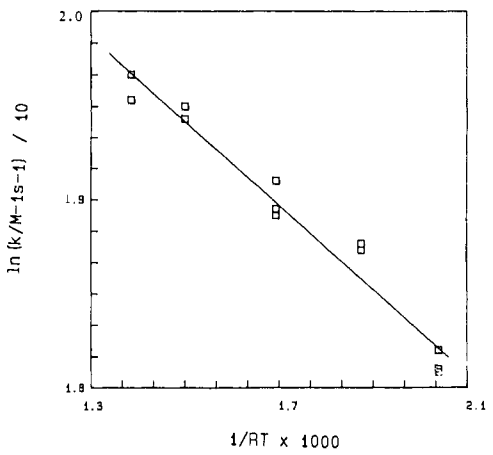

Figure 3. Arrhenius Plot for the reaction of *tert*-butyl radical with thiophenol determined from the laser photolysis of di-*tert*-butyl peroxide in the presence of tri-*tert*-butylphosphine and thiophenol.

To fit the differential equations (eq 18, 19) to the experimental absorbance data, an algorithm utilizing the Simplex[28] method was written to locate the best fit of k_6, the initial radical concentration, $[R^\bullet(0)]$, and ϵ using the estimates of k_7, k_8, and k_9. The Simplex program calculates a concentration–time profile by numerical integration of each set of varied, or assigned, rate constants k_6–k_9 and the initial radical concentration. For each set of rate constants generated during the Simplex fit, the maximum of the concentration profile is scaled to match the experimental absorbance curve with the factor ϵ (ϵ = molar extinction coefficient, l = irradiated path length). The sum of the squares of the residuals, $\sum(A_{calcd} - A_{expt})^2$, is minimized according to the Simplex scheme.[28] The calculation, executed with a DEC Microvax II, produces the values of k_6, initial radical concentration, and ϵl, which in turn yield the solid line of Figure 1.

The abstraction rate constant, k_6, calculated by this method, is relatively insensitive to the choice of k_9. The value of k_6 varies from 1.3×10^8 to 1.4×10^8 M^{-1} s^{-1} for variation of k_9 over the maximum probably range of error, approximately 30%[16] in calculation of k_9 by the Smoluchowski equation, $(2.7 \pm 0.9) \times 10^9$ M^{-1} s^{-1}. The value of k_6 changes by less than 1% for the maximum reasonable range of values of k_7 and k_8 because of the small

(27) The rate of self-termination of *tert*-butyl in nonane is an extrapolation between values determined in octane and decane by Schuh and Fischer. The cross-termination rate constant for butyl/PhS• termination value is the average value of the symmetric termination rate constants. A rate expression for self-termination of thiophenoxyl in nonane was estimated by using the von Smoluchowski equation, $2k_t = (8\pi/1000)\sigma p D_{AB}N$, where $\sigma = {}^1/_4$ (fraction of reacting singlet pairs), $p = 5.96 \times 10^{-8}$ cm (average of LeBas, Van der Waals, and Spernol–Wirtz reaction diameters), N = Avogadro's number, and D_{AB} is the diffusion coefficient of thiophenol in nonane, calculated from $D_{AB}\eta/T = k/6\pi r_A f$, where f is the microfriction factor of Spernol and Wirtz, $f = (0.16 + 0.4r_A/r_B)(0.9 + 0.4T_A^r - 0.25T_B^r)$. Reduced temperatures are given by $T_X^r = (T - T_X^f)/(T_X^b - T_X^f)$, where T_X^f and T_X^b are freezing and boiling points of species X = A, B. The radii in the microfriction factor term are given by $r_X = (3V_X(CHI)/4\pi N)^{1/2}$, where CHI = 0.74, the volume fraction for cubic closest-packed spheres. The resulting expression for the termination of thiophenoxyl is $\ln (2k_9/M^{-1}\ s^{-1}) = 26.8 - 2608/RT$. Other pertinent parameters are the freezing and boiling points of nonane, 222, 109.2 K, the boiling and freezing points of thiophenol, 258.4, 441.9 K, the temperature dependence of the viscosity of nonane, $\ln (\eta/cp) = -4.207 + 2246.44/RT$, the temperature dependence of the density of thiophenol = $1.353 - 9.41 \times 10^{-4}$ T (K), and the temperature dependence of the density of nonane = $0.972 - 8.64 \times 10^{-4}$ T (K): (a) Schuh, H.-H.; Fischer, H. *Helv. Chim. Acta* **1978**, *61*, 2130, 2463. (b) Schuh, H.-H.; Fischer, H. *Int. J. Chem. Kinet.* **1976**, *8*, 341.

(28) Caceci, M. S.; Cacheris, W. P. *Byte* **1984**, 340–362, and references therein.

participation of these reaction channels. The variation of k_6 is thus almost exclusively determined by the initial radical concentration and by k_9. By use of the rate constant k_6, $k_6 = 1.35 \times 10^8$ M^{-1} s^{-1}, determined from the Simplex fit of data of Figure 1, the systematic uncorrected error in the abstraction rate of data of Figure 1 is estimated to be +30%. Applying the termination correction reduces the error to around +5% for the experiment of Figure 1 (Table II). The initial radical concentrations were near 1×10^{-5} M for most of the determinations of this study. The residual errors in rate constants of this study are thus estimated to be reduced to approximately +5%, significantly less than the typical statistical error, ±30% (1σ).

The value of $\epsilon l = 2.02 \times 10^3$/M-cm, determined from the Simplex fit, yields $\epsilon = 806$/M-cm at 476 nm for the 2.5-cm irradiated path length from Figure 1 data. Direct calculation of $2k_9/l\epsilon$ from the experimental absorbance curve varies for the case of Figure 1 by 1% from the Simplex value (Table II), with the difference arising from calculating $2k_9/l\epsilon$ from the decay portion of Figure 2 compared to the Simplex fit, which utilizes the entire curve following the excimer pulse.

Rate Constants and Arrhenium Parameters for Hydrogen Abstraction from Thiophenol. The rate constants for abstraction of hydrogen from thiophenol are clustered around 1.3×10^8 M^{-1} s^{-1} at 298 K. No steric effect is apparent in the progression from primary to tertiary alkyl radicals. The relative insensitivity of abstraction rates to radical structure and the low temperature dependence suggest that the thiophenol abstraction reactions provide suitably nonselective hydrogen abstraction standards applicable to a broad variety of substituted alkyl radicals with little error due to changes in steric and electronic character. The activation barriers for hydrogen abstrction from thiophenol (1.5–1.7 kcal/mol) are ~2 kcal/mol lower than those for abstraction from tributylstannane.[14] The rates of reaction of alkyl radicals with thiophenol are ~1 order of magnitude slower than diffusion control, exceeded only by alkyl radical abstraction rates from transition-metal hydrides.[29]

The Arrhenius A factors [log (A/M^{-1} s^{-1}); Table I] vary from 9.1 to 9.4. These values are higher than observed for hydrogen transfer between hydrocarbons and carbon-centered radicals (log (A/M^{-1} s^{-1}) = 8.5 ± 0.5[20]) but similar to values for other highly exothermic hydrogen transfers from metal hydrides [Bu_3SnH[14], $Me_5CpMo(CO)_3H$[29]]. The accuracy of the range of A factors was confirmed by the careful determination by Newcomb and Glenn[12] of the relative rate expression for rearrangement of the cyclopropylmethyl radical in competition with hydrogen abstraction from thiophenol: log ((k_1/k_6)/M) = (3.6 ± 0.14) − (5.1 ± 0.2)/θ, $\theta = 2.3RT$ kcal/mol. The A factor for the cyclopropylmethyl radical ring opening can be accurately estimated by difference methods[4,20] (see below). The predicted value, $10^{13.0}$ s^{-1}, when combined with Newcomb and Glenn's expression, predicts an A factor of $10^{9.4}$ M^{-1} s^{-1}, in excellent agreement with the observed A factor for the n-butyl radical (Table I), and in good agreement with the average A factor, $10^{9.3}$ M^{-1} s^{-1} for all of the reactions of Table I.

The A factor for the cyclopropylmethyl radical ring opening reaction was estimated for use with Newcomb and Glenn's relative rate expression to test the accuracy of abstraction A factors of Table I. Difference methods[20] are particularly suited for calculation of the entropy of activation of the cyclopropylmethyl ring opening, due to the minor, well-defined changes in geometry, bonding, and molecular vibrations in the transition structure. The entropy changes are defined by contributions from reaction path degeneracy (R ln 2, 1.4 eu) and reduction in symmetryt (R ln 2, 1.4 eu, for $\sigma = 2 \rightarrow \sigma^\ddagger = 1$) compensated partially by loss of 3.9 eu[20] for conversion of the cyclopropylmethyl methylene-hindered rotation (1 kcal/mol predicted by AM1[30]) to an olefin torsional vibration of 420 cm^{-1}.[30] (A methylene rotational barrier of 0.5 kcal/mol, a value more typical of C_α–C_β rotational barriers,[31] would increase the entropy loss of the methylene rotor to 4.1 eu). Loss of the ca. 1600 cm^{-1} C–C ring stretch[30] to the transition state results in negligible entropy loss. All other changes in translational, vibrational, and rotational entropy are negligible. For a rotational barrier of 1 kcal/mol, $\Delta S^\ddagger = -1.1$ eu, and $A = (ekT_m/h)e^{\Delta S^\ddagger/R} = 10^{13.23}e^{\Delta S^\ddagger/R} = 10^{13.0}$ for $T_m = 298$ K. For a 0.5 kcal/mol methylene rotational barrier, $\Delta S^\ddagger = -1.4$ eu, and $A = 10^{12.9}$. Thus, the A factor for the cyclopropylmethyl rearrangement determined by combining the data of Newcomb and Glenn[12] and the rate expression for abstraction of hydrogen by the n-butyl radical, $10^{13.0}$, provides verification of the accuracy of the range of abstraction A factors of Table I. A full discussion of the rate expression recommended for the cyclopropylmethyl rearrangement is provided in the accompanying paper.[12] The barrier of 1 kcal/mol predicted by AM1 for the methylene rotation indicates negligible resonance stabilization of the cyclopropyl radical, supporting the validity of using the n-butyl rate expression of Table I as a basis reaction for this rearrangement.

Summary. This work and a previous paper[8] have provided absolute rate expressions for the reaction of primary, secondary, tertiary, and benzyl radicals with thiophenol suitable for use as rate standards for calibration of alkyl[12] and benzl[32] radical clock reactions. A simple method for extension of the kinetic absorption spectroscopic method of measurement of atom abstraction rates to operate at radical concentrations of a factor of ca. 10 higher than normal concentrations has been described. A new, accurate rate expression for the cyclopropylmethyl radical rearrangement has been presented. The value of thiophenol as a standard competitive abstraction reaction is further enhanced by the results of Newcomb and Glenn, which reveal that thiophenol can participate in a chain reaction using the Barton precursor to the alkyl radical.[12]

(29) The rate expression for reaction of the hex-5-enyl clock radical with pentamethylcyclopentadienyltricarbonylmolybdenum hydride ($Me_5CpMo(CO)_3H$) is given by log (A/M^{-1} s^{-1}) = 9.27 ± 0.04 − (1.35 ± 0.11)/θ, $\theta = 2.3RT$ kcal/mol: Franz, J. A.; Linehan, J. C.; Alnajjar, M. S., unpublished results.

(30) AM1 (UHF) calculations of the cyclopropylmethyl ground state and transition state and the cyclopropylmethyl methylene rotational barrier were carried out with the AMPAC molecular orbital program package, Version 1.00: Stewart, J. J. P. *QCPE No. 566*. Dewar, M. J. S.; Zoebisch, E. F.; Healy, E. F.; and Stewart, J. J. P. *J. Am. Chem. Soc.* **1985**, *107*, 3902–3909. For cyclopropylmethyl radical (atom numbering: C4–C1–C2–C3•–(H10)(H11)), the methylene rotational barrier was found to be 1.02 kcal/mol for dihedral angles H10–C3–C2–C1 of 234° and H11–C3–C2–C1 of 54.8° ($\Delta H^\circ_{f,298}$ = 44.32 kcal/mol at the maximum of the rotational profile compared to the ground state, for which the H10–C3–C2–C1 dihedral is 145.3°, H11–C3–C2–C1 is −34.7°, and $\Delta H^\circ_{f,298}$ = 43.3 kcal/mol (g.s.). An AM1 UHF vibrational calculation for the cyclopropylmethyl ground state and the ring-opening transition state reveals the lowest lying vibration of the ground state to be the methylene internal rotation (130.99 cm^{-1}). This vibration becomes a 420.906 cm^{-1} methylene torsion in the ring-opening transition state. Multiplying this value by 0.92 for comparison with experiment gives 387 cm^{-1}, corresponding to an entropy content of 0.3 eu (ref 22). A 1633 cm^{-1} (× 0.92 = 1502 cm^{-1}) stretching frequency, which is a ring breathing motion involving simultaneous stretch of the three ring C–C bonds and is the only vibration that involves a C1–C2 stretch, is lost to the transition state (−888.9 cm^{-1}). The ring C–C bond length of the ground state, 1.512 Å, becomes 1.842 Å in the transition state. AM1 predicts a 12.7 kcal/mol activation enthalpy for cyclopropylmethyl ring opening (heat of formation of the transition-state radical = 55.95 kcal/mol). The transition-state dihedral angle H10–C3–C2–C4 is 178.9°, and H11–C1–C2–C4 is −2.6°, showing the near planarity of the evolving olefin. For a review of ab initio and semiempirical calculations of cyclopropylmethyl see: Wuenemoen, K.; Borden, W. T.; Davidson, E. R.; Feller, D. *J. Am. Chem. Soc.* **1985**, *107*, 5054. Of the calculations carried out on this system, only one ab initio result, carried out at the UHF 4-31G level, provides an activation enthalpy within 3 kcal/mol of kinetic results: Hehre, W. J. *J. Am. Chem. Soc.* **1973**, *95*, 2643. For recent ab initio calculations of rotational barriers, see: Claxton, T. A.; Graham, A. M., *J. Chem. Soc., Faraday Trans. 2*, **1988**, *84*, 121–134, and references therein. Ab initio calculation of the cyclopropylmethyl rotational barrier: Delbecq, F. *THEOCHEM*, **1986**, *29(1-2)*, 65–75; *Chem. Abstr.* **1986**, *105*, 133031u.

(31) C_α–C_β barriers, n-propyl, 0.4 kcal/mol; isobutyl, 0.3 kcal/mol: Krusic, P. J.; Meakin, P.; Jesson, J. P. *J. Phys. Chem.* **1971**, *75*, 3438. Recently measured barriers for 2-(cycloalkenyl)ethyl barriers lie between 0.12 and 0.4 kcal/mol: Walton, J. C. *J. Chem. Soc., Perkin Trans. 2* **1987**, 1809–1813, and references therein.

(32) Franz, J. A.; Alnajjar, M. S.; Barrows, R. D.; Kaisaki, D. A.; Camaioni, D. M.; Suleman, N. K. *J. Org. Chem.* **1986**, *51*, 1446.

Acknowledgment. We are grateful to Professor M. Newcomb for sharing the cyclopropylmethyl rearrangement data prior to publication.

Supplementary Material Available: Tabulations of kinetic data and Arrhenius plots for the entries of Table I and Fortran data acquisition and reduction programs for collection and treatment of raw transmittance data including correction for second-order termination (13 pages). Ordering information is given on any current masthead page.

A Convenient Method for Kinetic Studies of Fast Radical Rearrangements. Rate Constants and Arrhenius Function for the Cyclopropylcarbinyl Radical Ring Opening

Martin Newcomb* and Anne G. Glenn

Contribution from the Department of Chemistry, Texas A&M University, College Station, Texas 77843. *Received May 5, 1988*

Abstract: An indirect method for studying the kinetics of radical rearrangements employing *N*-hydroxypyridine-2-thione esters as radical precursors and hydrogen atom transfer from thiophenol as the basis trapping reaction is demonstrated in a study of an archetypal fast radical reaction, the cyclopropylcarbinyl radical ring opening. Rate constants measured over the temperature range −37 to 50 °C gave a temperature-dependent function for the ring opening of $\log (k/s^{-1}) = (13.0 \pm 0.14) - (6.8 \pm 0.2)/\theta$ and a rate constant for ring opening at 25 °C of 1.0×10^8 s^{-1}. The kinetic values from this work were combined with rate data from low-temperature ESR studies and higher temperature nitroxyl radical trapping studies to give an Arrhenius function of $\log (k/s^{-1}) = 13.15 - 7.05/\theta$ that is recommended for calculations of rate constants for the title ring opening.

The measurement of carbon radical reaction rate constants can be accomplished by direct or indirect methods. For rearrangements of alkyl radicals that contain no chromophore and are present in low concentrations, indirect kinetic measurements, where the reaction of interest competes with a reaction with a known rate constant, are common, and the "tin hydride" method has been the most exploited indirect method. Accurate rate constants for second-order reactions of Bu_3SnH with several simple alkyl radicals are available,[1] and reactions of Bu_3SnH are relatively insensitive to carbon radical structure. These two features permit one to estimate with confidence the rate constants for radical reactions with Bu_3SnH, and some of the most widely used "radical clocks" such as 5-hexenyl have been calibrated by this approach.[2] However, the tin hydride method has been limited in the scope of radicals and in the range of rate constants that could be studied. The former limitation (usually requiring an alkyl halide precursor for the desired radical) was relieved by the development of *N*-hydroxypyridine-2-thione esters R-PTOC, where PTOC = [((1*H*)-pyridine-2-thione)oxy]carbonyl, by Barton[3] which have been shown to be excellent radical precursors in indirect kinetic studies.[4,5] The latter limitation is an inherent property of the tin hydride; very fast radical rearrangements ($k_r > 1 \times 10^8$ s^{-1} at 25 °C) will overwhelm the trapping reaction ($k_H = 2.4 \times 10^6$ M^{-1} s^{-1} at 25 °C).[1] Since Barton's alkyl-PTOC compounds participate in radical chain reactions with a variety of radicals including thiyl radicals, the use of these precursors permits alternative basis reactions for the indirect measurement of fast radical rearrangements. With accurate values for the rate constants for hydrogen atom transfer from PhSH now available,[6] we demonstrate this convenient method in a kinetic study of the ring opening of the cyclopropylcarbinyl radical **1** to the 3-butenyl radical **2** (Scheme I). Our results, measured over the temperature range −37 to 50 °C, give a reasonable Arrhenius function that is independently consistent with measurements of k_{12} from −145 to 122 °C.

Scheme I

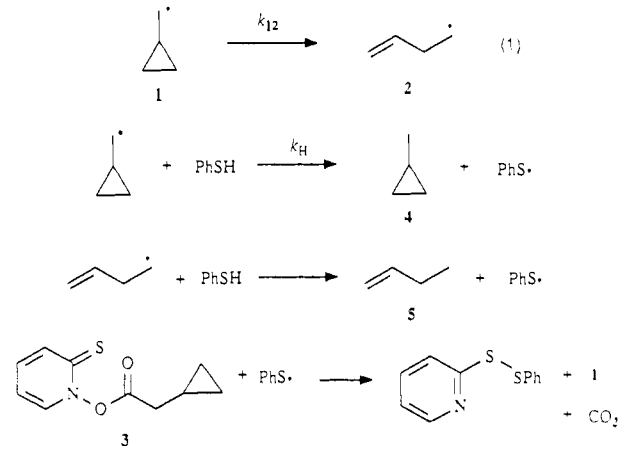

The ring opening of the cyclopropylcarbinyl radical to the 3-butenyl radical (eq 1 in the scheme) is a fast radical rearrangement that holds a position of distinction in mechanistic studies involving "radical clocks" and "mechanistic probes". Numerous studies have employed potential precursors of this radical or its analogues in attempts to implicate radical intermediates in a reaction pathway by detection of the products from the radical ring opening, and the rate constant for the conversion in eq 1 is probably the most often quoted fast radical rearrangement velocity. Rate constants for this ring opening were

(1) Johnston, L. J.; Lusztyk, J.; Wayner, D. D. M.; Abeywickreyma, A. N.; Beckwith, A. L. J.; Scaiano, J. C.; Ingold, K. U. *J. Am. Chem. Soc.* **1985**, *107*, 4595.
(2) Griller, D.; Ingold, K. U. *Acc. Chem. Res.* **1980**, *13*, 317.
(3) Barton, D. H. R.; Crich, D.; Motherwell, W. B. *Tetrahedron* **1985**, *41*, 3901.
(4) Newcomb, M.; Park, S.-U. *J. Am. Chem. Soc.* **1986**, *108*, 4132.
(5) *N*-hydroxypyridine-2-thione esters are also useful radical precursors for ESR studies: Ingold, K. U.; Lusztyk, J.; Maillard, B.; Walton, J. C. *Tetrahedron Lett.* **1988**, *29*, 917.
(6) Franz, J. A.; Bushaw, B. A.; Alnajjar, M. S. *J. Am. Chem. Soc.*, preceding paper in this issue.

0002-7863/89/1511-0275$01.50/0